JOURNAL OF MATERIALS SCIENCE 26 (1991) 1032–1038

Effect of salt-water fog on fatigue crack growth behaviour of 7050 aluminium alloy in different orientations

R. GÜRBÜZ*, M. DORUK*, W. SCHÜTZ‡
* *Department of Metallurgical Engineering, Middle East Technical University, Ankara, Turkey*
‡ *Industrieanlagen-Betriebsgesellschaft mbH., Ottobrunn, FRG*

The fatigue crack growth behaviour of 7050 T73651 high strength aluminium alloy that was originally developed for the aircraft industry was investigated in this study. The tests were conducted by using C–T specimens machined in six orientations under the action of constant amplitude sinusoidal load cycles. The tests were first carried out in laboratory air and then repeated in salt-water fog of a 5% NaCl solution to observe the effect of the environment on the fatigue crack growth behaviour. The experimental results showed that the fatigue life, maximum stress intensity range and the fatigue crack growth rate of the specimens were seriously affected by the environment. The severity of the effect, on the other hand, was observed to be dependent on the orientation. The strongest orientation was determined to be L–S, while the weakest was S–L.

1. Introduction

The high strength, high modulus and low weight of age-hardenable 7000 series aluminium alloys make them ideal for use in aircraft construction. Their use is, however, limited especially in marine atmospheres because of their susceptibility to stress corrosion cracking, exfoliation and intergranular corrosion [1].

The corrosion fatigue properties of 7050 aluminium alloys have therefore gained great importance in recent years because of their extensive use in the form of plates in many components of primary load carrying structures of aircraft flying in marine atmospheres. Military aircraft especially may continuously be exposed to splashing of sea-water, by wind or to salt-water spray from the sea during their flight at low altitudes over the sea (close to the sea surface) and during their taking off or landing on the deck of an aircraft carrier. In addition, the sea-water which is condensed on the skin of those aircraft when they are at rest on the deck of the carrier may cause the structural parts to be pre-exposed to aggressive salt-water.

This research was therefore planned to extend the available data about air and corrosion fatigue behaviour of 7050 aluminium alloy in marine atmosphere. A pre-exposure in 5% NaCl solution and salt-water fog environment was selected for the simulation of environmental conditions of military aircraft on carriers. Another aim of the research was to determine the directional distribution of properties in a thick plate.

2. Experimental details

2.1. Testing material and specimen

The testing material was a cold-rolled plate of 7050 T73651 aluminium alloy with the dimensions of 200 × 100 × 11 cm^3. The chemical composition of the alloy in weight percentages is given in Table I.

The T73651 temper applied to the plate by the manufacturer was solutionizing at 477 °C followed by double ageing at 121 °C for 24 h and at 163 °C for 24 h. It was found that about one third of the microstructure was made up of recrystallized and two thirds of it was made up of polygonized grains. Very fine precipitates were observed to be evenly distributed throughout the structure, whereas larger intermetallic compounds were mostly detected among the recrystallized grains. The flattening of the recrystallized grains in the short transverse direction and their elongation in the rolling direction were found to be significant (Fig. 1).

The statistical stress–strain properties of the plate in different directions determined in a previous work are given in Table II [2].

The distribution of the fracture toughness was reported to be homogeneous throughout the plate including the thickness direction. Significant differences were, however, seen to exist in fracture toughness values in different orientations. The plane strain fracture toughness, K_{IC}, values determined in four orientations are given in Table III [2].

The dimensions and the six different orientations of C–T specimen manufactured according to ASTM E 647-83 standards [3], are shown in Fig. 2.

2.2. Testing equipment

All tests were conducted on a closed-loop, servo-hydraulic MTS testing machine. A salt-water fog system was manufactured for conducting the corrosion

0022–2461/91 $03.00 + .12

TABLE I The chemical composition of 7050 T73651 aluminium alloy in weight percentages

Zn	Mg	Cu	Zr	Ti	Cr	Mn	Si	Fe	Al
6.20	2.25	2.30	0.12	0.06	0.04	0.10	0.12	0.15	Rest

fatigue experiments. The schematic view of the fog producing system is illustrated in Fig. 3.

2.3. Crack length measurement

Crack lengths were measured directly on the surfaces of the C–T specimen by attaching electrical crack gauges with a sensitivity of $\pm$ 0.02 mm. The average of the two values was calculated and used in the evaluation of experimental data. After the fracture, cracks were examined for departure from crack plane in accordance with ASTM E 647-83 [3] standard test method. The through thickness final crack lengths were determined using a vernier at three points across the thickness of the failed specimens.

2.4. Testing procedure and programme

Four specimens in each orientation were machined to study the effect of salt-water fog on fatigue crack growth behaviour. Two of the specimens were tested in laboratory air and the other two in salt-water fog.

All specimens to be tested in laboratory air were first precracked by subjecting them to constant amplitude sinusoidal load cycles with a frequency of 10 Hz to obtain an infinitely sharp fatigue precrack that satisfies the requirements of the ASTM E 647-83 standard.

Laboratory air tests were conducted by subjecting the specimens to a constant load amplitude sinusoidal wave with a frequency of 2 Hz. The maximum amplitude of the load cycle and the stress ratio, R, were selected as 5000 N and 0, respectively. The temperature of the laboratory air was kept constant at 25 °C. All tests were conducted until the failure of specimens.

The specimens to be tested in salt-water fog were first immersed into a 5% NaCl solution for 72 h to simulate the flight deck environments of an aircraft carrier. They were then precracked under the same loading conditions of the specimens tested in laboratory air.

The corrosion fatigue tests were conducted by subjecting those specimens to a constant load amplitude sinusoidal wave with a frequency of 0.5 Hz. The maximum load amplitude and the stress ratio were the same as used in air tests. Testing was performed in the salt-water fog chamber until fracture. Salt spray was produced continuously during these tests. A 5% NaCl solution acidified by H_2SO_4 to a pH value of 4 was used for producing the salt-water spray.

The high strength steel fasteners that hold the specimens were coated with zinc to minimize the effect of

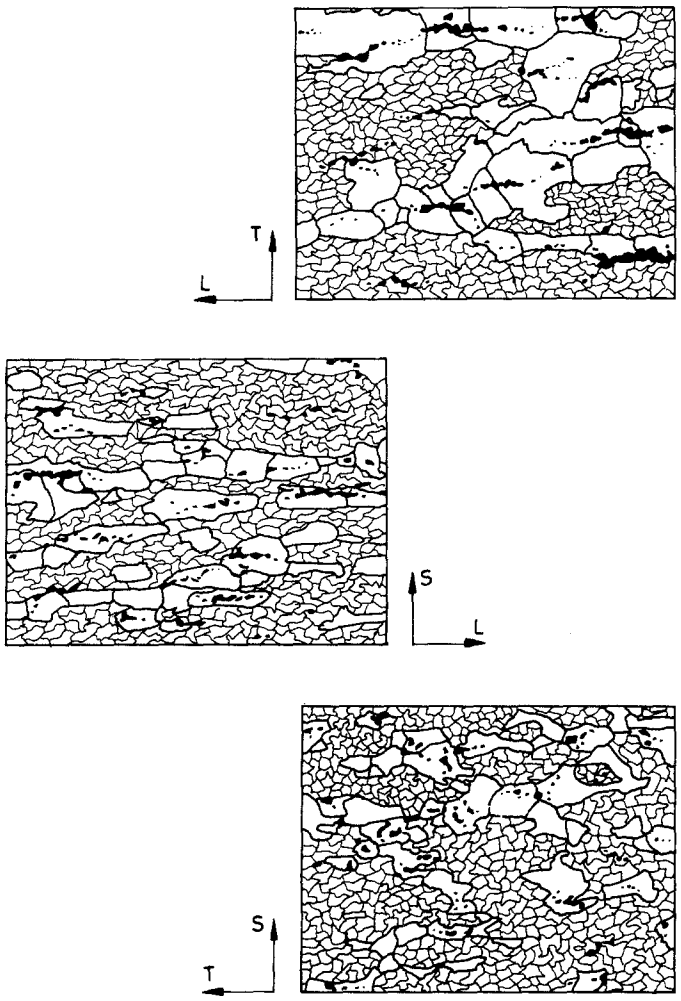

Figure 1 The microstructures of 7050 T73651 aluminium plate in three directions. Large grains are recrystallized.

TABLE II Mechanical properties of 7050 T73651 aluminium rolled plate in three directions

Direction	UTS ($N mm^{-2}$)	σ_y ($N mm^{-2}$)	E ($N mm^{-2}$)	Elongation (%)
L	510	447	72200	10
LT	519	444	73300	9
ST	502	423	72800	7

TABLE III Plane strain fracture toughness, K_{IC}, values of 7050 T73651 aluminium plate in four orientations

Orientation	L–T	T–L	S–T	S–L
K_{IC} ($N mm^{-3/2}$)	1215	966	957	865

galvanic coupling of the fasteners and the specimen. The alignment quality of the testing machine and the specimen-pin–clevis assembly were carefully checked before conducting the experiments.

2.5. Determination of crack growth rates

The average crack length, a, against elapsed stress cycles, N, data have been recorded during the experiments at intervals recommended by ASTM E 647-83. These data were then evaluated by using a seven-point incremental polynomial technique to determine the crack growth rate, da/dN. Third-degree polynomials were then fitted to the log da/dN against log ΔK data to predict the fatigue crack growth rates.

3. Results and discussion

Experimental results showed that there were three significant effects of the environment on the fatigue crack growth behaviour of the alloy tested:

(i) a decrease in fatigue life
(ii) a decrease in maximum stress intensity range
(iii) an increase in crack growth rate.

TABLE IV Maximum stress intensity range values and the fatigue lives in air and salt-water fog in six orientations. ΔK_{max} values in L–S orientation could not be determined exactly because the crack length, a, exceeded the maximum working range (20 mm) of the crack gauges used in crack length measurements

Orientation	ΔK_{max} ($N mm^{-3/2}$)		Fatigue life (cycles)	
	Air	Salt	Air	Salt
L–S	> 1351.13	> 1351.13	35750	35000
S–L	488.40	447.30	22000	11750
L–T	761.28	704.47	33750	11500
T–L	624.42	561.66	26500	15500
T–S	1099.13	724.96	47000	22000
S–T	550.91	470.28	27500	18750

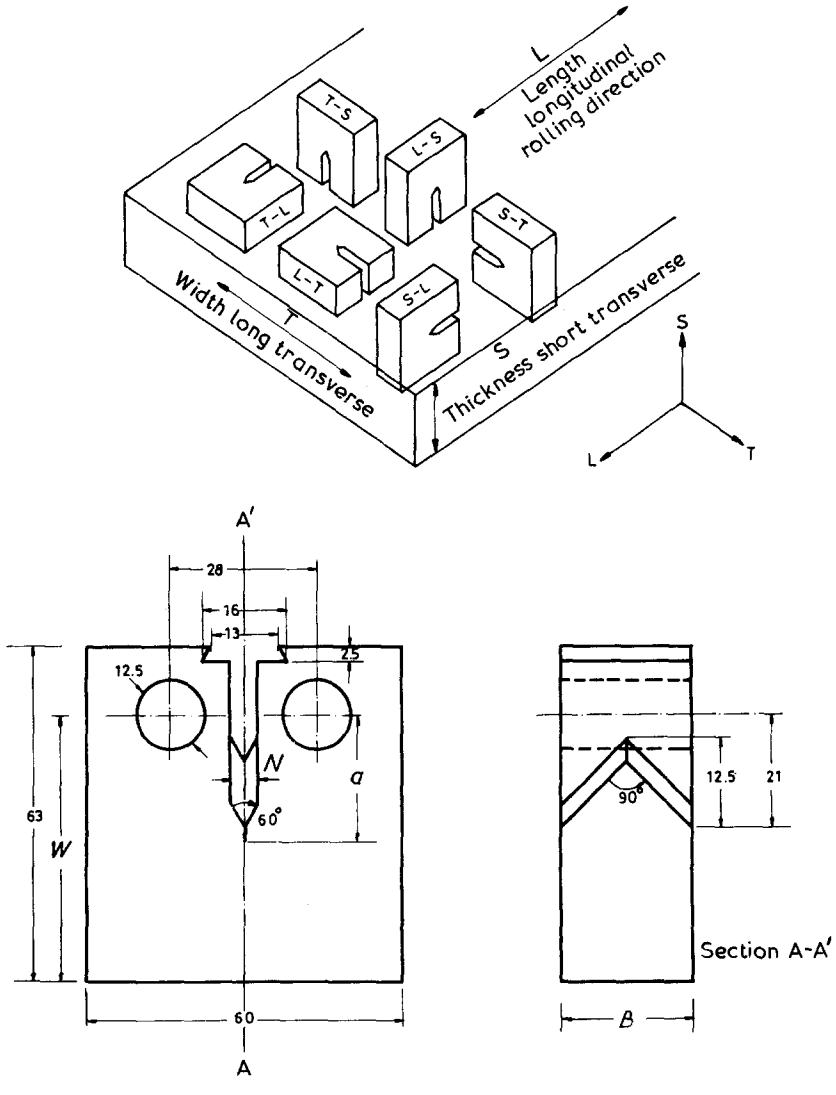

Figure 2 The dimensions and the orientations of the C–T specimen used in experiments. $W = 50$ mm, $B = 25$ mm, $N = W/10 = 5$ mm, a crack length.

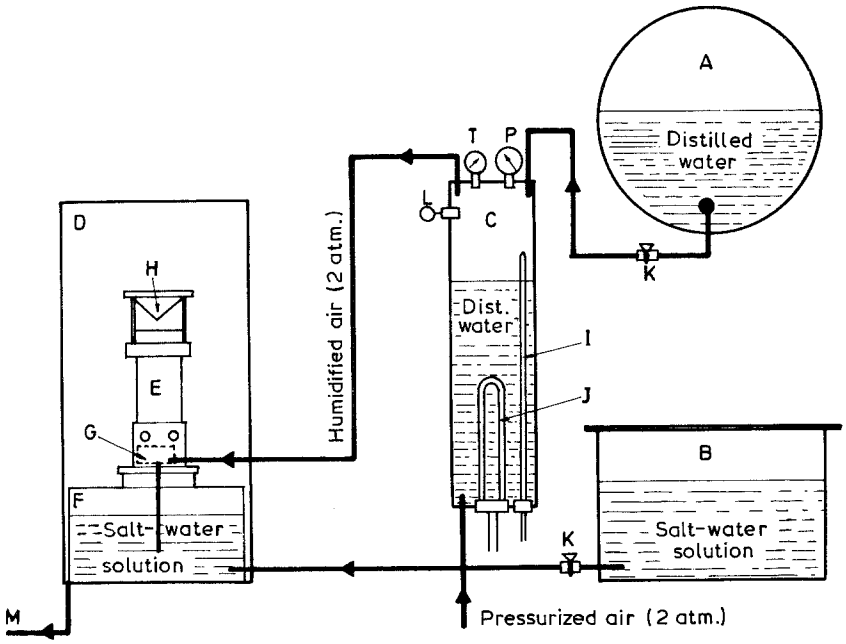

Figure 3 The schematic view of the salt-water fog system. A: Distilled water container, B: 5% NaCl (pH = 4) salt-water container, C: Humidifying tower, D: Salt-water fog chamber, E: Spraying tower, F: Salt water container of the chamber, G: Nozzle, H: Fog deflector, I: Thermocouple of the temperature controller, J: Heater, K: Valves, L: Pressure control valve, M: Discharging hose for the condensed salt-water, P: Pressure gauge, T: Temperature gauge.

The severity of the environmental effect, on the other hand, was determined to be strongly dependent on orientation.

3.1. Fatigue life

A definite decrease was observed in the fatigue life of the specimens tested in salt-water fog compared to those tested in laboratory air (Table IV). This decrease was observed for all orientations but in different proportions. The severity of the effect was the highest in L–T having a fatigue life in air 2.50 times higher than that in salt-water fog. The L–S orientation, however, seemed to have the highest resistance against the aggressive effect of the environment showing almost no decrease in fatigue life.

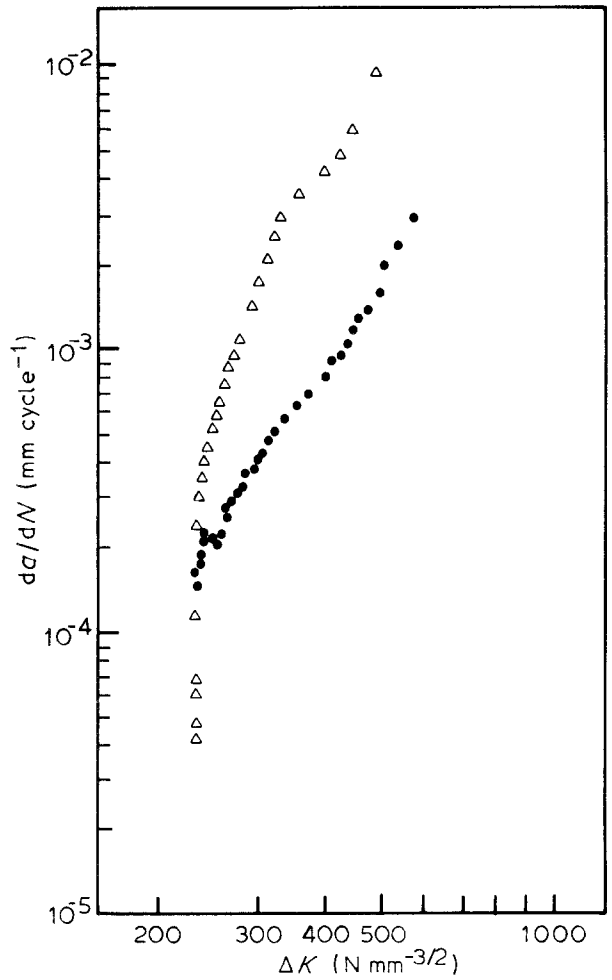

Figure 4 da/dN against ΔK plot of L–T specimens tested in air (•) and salt-water (△) fog.

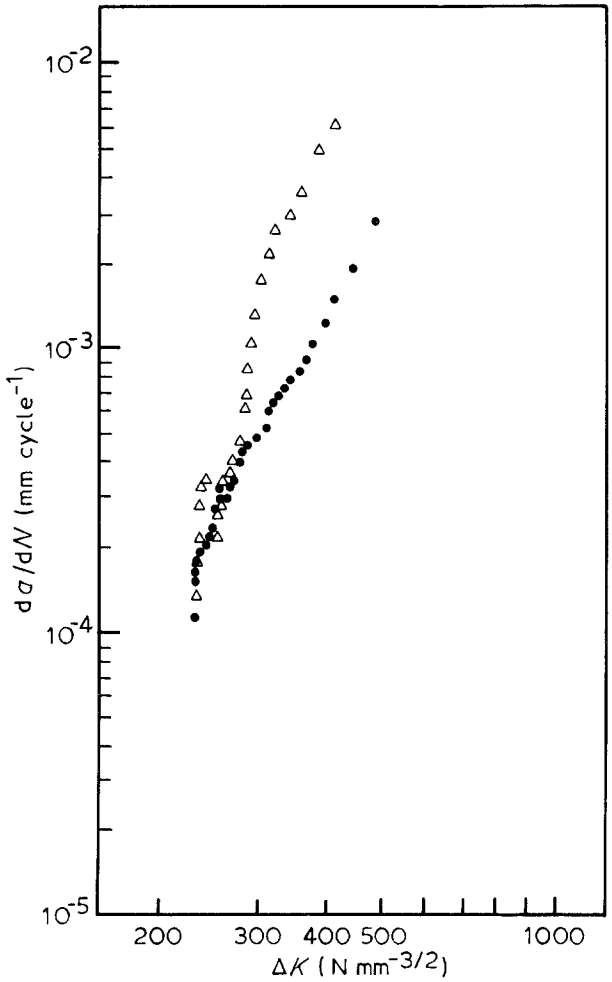

Figure 5 da/dN against ΔK plot of T–L specimens tested in air (•) and salt-water (△) fog.

3.2. Maximum stress intensity range, ΔK_{max}

ΔK_{max} is the stress intensity range calculated by using the final crack length determined just before fast fracture and the maximum load of the stress cycle. It is observed from Table IV that ΔK_{max} decreases in salt-water fog to a varying extent depending on the orientation. The effect of the environment on ΔK_{max} is maximum in the T–S and minimum in the L–S orientation. In T–S the amount of decrease in ΔK_{max} is about 34% whereas no difference can be observed in L–S. The differences for the other four orientations lie between these two values being 15% for S–T, 10% for T–L, 8.4% for S–L and 7.5% for L–T.

If the stress ratio is zero and the fracture is assumed to occur at the maximum of the final load cycle, ΔK_{max} can be considered to be directly related to K_{IC} of the material which is independent of the environment. Our findings about ΔK_{max}, however, have shown some differences between air and corrosion fatigue tests. Slight differences in five orientations (all except T–S) may be explained by the hydrogen embrittlement mechanism originating from the environment at the crack tip. The presence of such a mechanism creates a hydrogen diffused region ahead of the crack tip. The hydrogen penetration distance increases with decreasing frequency. The testing frequency of the corrosion fatigue tests in this research was low enough (0.5 Hz) to permit the diffusion of hydrogen and to form a hydrogen penetration distance ahead of the crack tip. In such a case, the real crack length may be considered to be extended and it should be calculated by adding the hydrogen penetration distance to the measured crack length from the surfaces.

3.3. Crack growth rate

It is definite from crack growth rate diagrams (Figs 4 to 9) that the existence of salt water fog increases the crack growth rates in varying amounts depending on the orientation and ΔK level.

For relatively low crack growth rates (less than 2×10^{-4} mm cycle^{-1}), almost no effect of the environment is observed. As can be seen from Figs 4 to 9, for the data points corresponding to da/dN values lower than 2×10^{-4} mm cycle^{-1} and to ΔK values lower than 240 N mm$^{-3/2}$, air and salt water fog results do almost coincide with each other. This fact can be verified directly for the orientations of T–L, L–S, S–T and T–S from Figs 5, 6, 8 and 9, respectively. The same kind of behaviour may, however, be expected for the other two orientations L–T and S–L after performing some extrapolations.

When the crack growth rate exceeds the value of 2×10^{-4} mm cycle^{-1}, the salt-water fog begins to become effective on crack growth rates. The extent of this effect, however, seems to be dependent on the orientation. From Figs 4 to 9, it can be seen that the

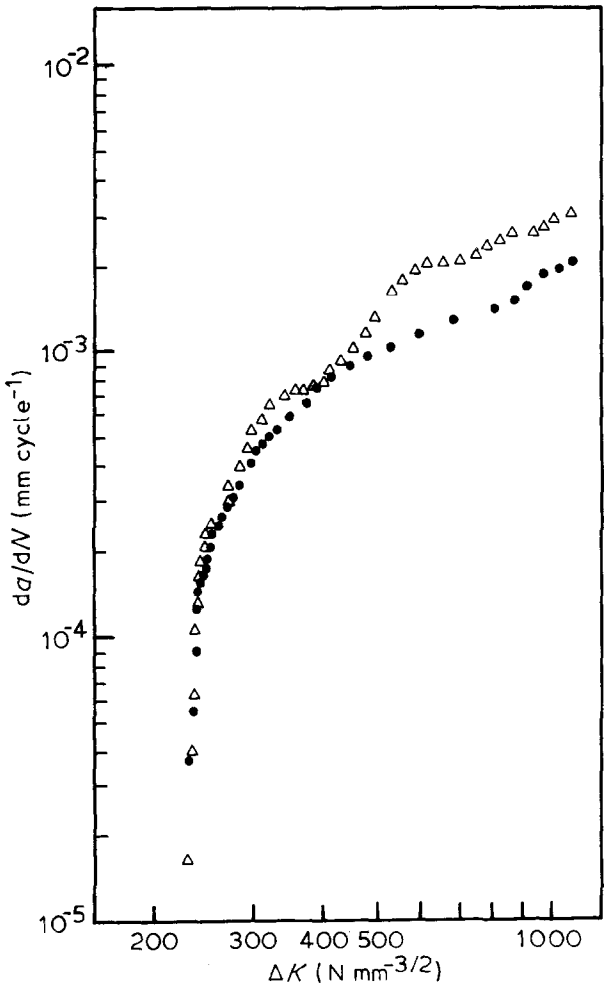

Figure 6 da/dN against ΔK plot of L–S specimens tested in air (•) and salt-water (△) fog.

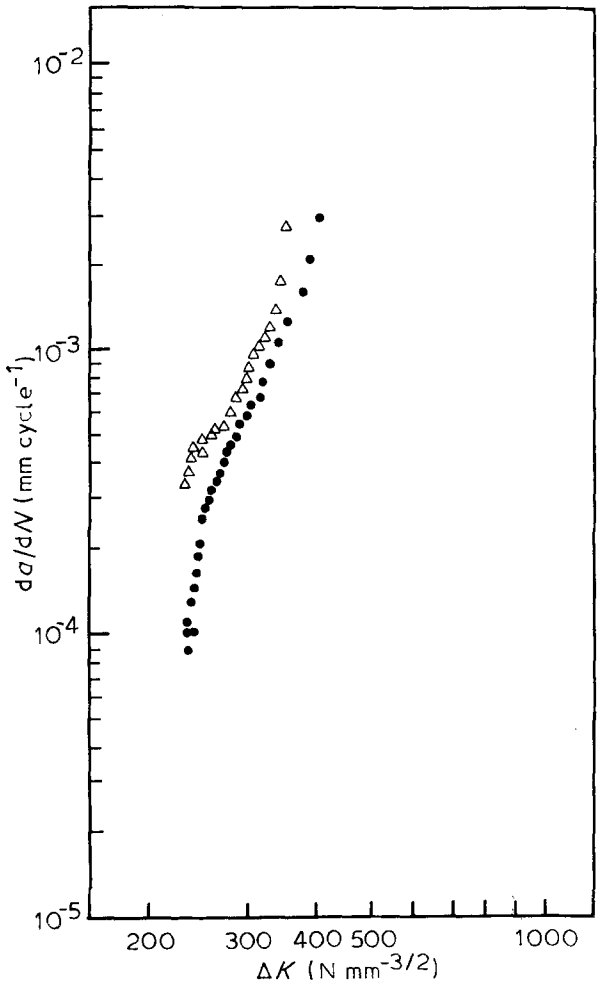

Figure 7 da/dN against ΔK plot of S–L specimens tested in air (•) and salt-water (△) fog.

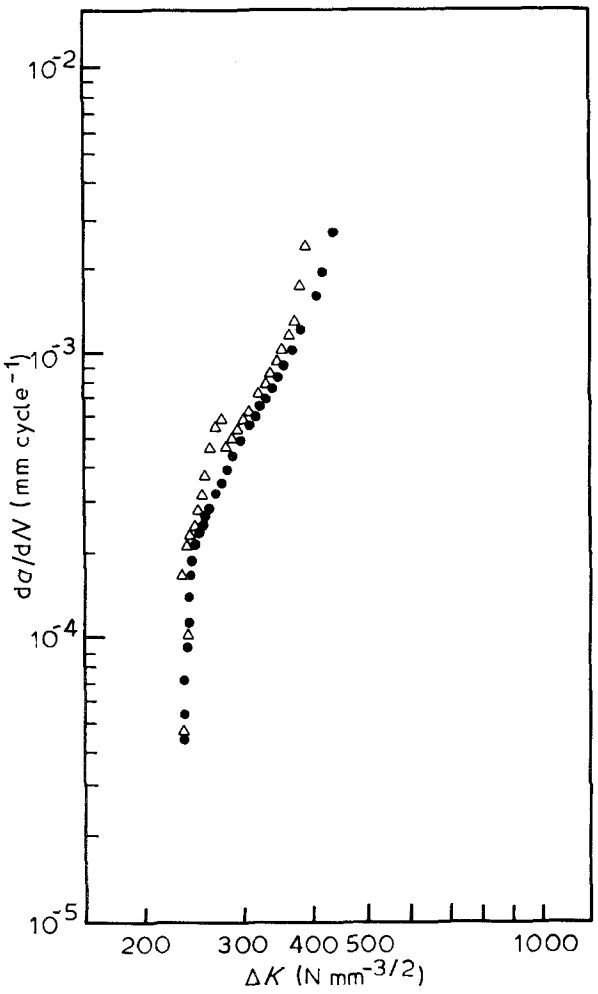

Figure 8 da/dN against ΔK plot of S–T specimens tested in air (•) and salt-water (△) fog.

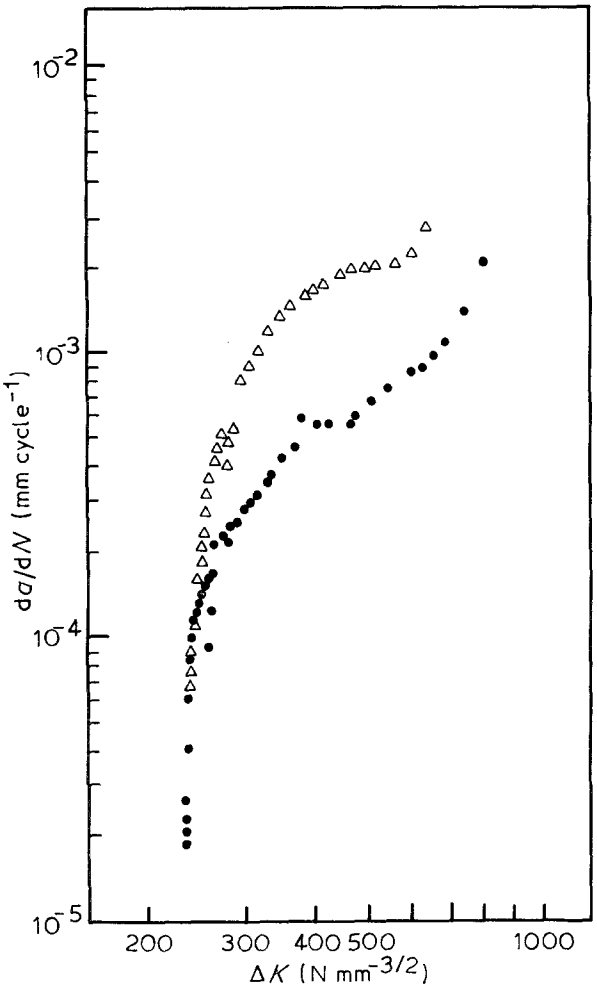

Figure 9 da/dN against ΔK plot of T–S specimens tested in air (•) and salt-water (△) fog.

effect is noticeably high for the orientations L–T, T–L and T–S. On the other hand, it is relatively low for the L–S and S–L and almost ignorable for the S–T orientations. In the stress intensity range between 300 and 500 N mm$^{-3/2}$, it can be calculated that salt-water fog causes an average of 4.5 times faster growth of fatigue cracks compared to air specimens for the orientations of L–T and T–L. This factor is slightly less for T–S and is about 3. For the other three orientations L–S, S–L and S–T, the factor is calculated to be 1.4, 1.5 and 1.2, respectively.

It is seen that the effect of salt-water fog on the fatigue crack growth rate is most marked at intermediate ΔK values especially for the orientations L–T, T–L and T–S. However, a decrease in the influence of environment is usually expected at high ΔK levels where ΔK approaches the fracture toughness [5–8] for most of the cases. The approaching of fatigue and corrosion fatigue curves is explained by observation that at such high ΔK levels a major portion of the crack growth is due to void nucleation and void coalescence. This mode of crack extension does not depend on the external conditions since most of it occurs inside the material just ahead of the crack front, where the environment cannot reach. This type of fracture—voids and dimples—was observed in SEM examinations at high ΔK levels in almost all fracture surfaces. It is on the contrary observed in our plots that the influence of the environment is usually higher at high ΔK levels and the air and salt curves do not approach each other.

The deterioration of the corrosion fatigue specimens during pre-exposure may create such an effect. Some recent experimental programs on 7000 series aluminium alloys indicated that pre-corrosion experiments in NaCl solution followed by tests in air resulted in significant decreases in fatigue resistance [9]. The decreases in ΔK_{max} may be in agreement with this finding.

Figs 10 and 11 briefly summarize the fatigue crack growth behaviour of 7050 aluminium alloy in air and in salt-water fog for six different orientations. Fig. 10 shows clearly that the air fatigue resistance of each orientation is different. The most resistant orientations are L–S and T–S. L–S has the highest ΔK_{max} and the lowest da/dN for ΔK values greater than 700 N mm$^{-3/2}$. ΔK_{max} of T–S, on the other hand, is still higher than the other four orientations and it has the lowest da/dN for ΔK less than 700 N mm$^{-3/2}$. S–L has the lowest resistance to air fatigue crack growth showing the highest da/dN at any ΔK level and the smallest value of ΔK_{max}.

The salt-spray fog comparison (Fig. 11) of the orientations gives similar results, again, L–S emerges as the strongest orientation. S–L seems to be the weakest with minimum ΔK_{max}. The crack growth rates of L–T and T–L are also very high with respect to others, the first reaching a value of 10^{-2} mm cycle^{-1} near fast fracture.

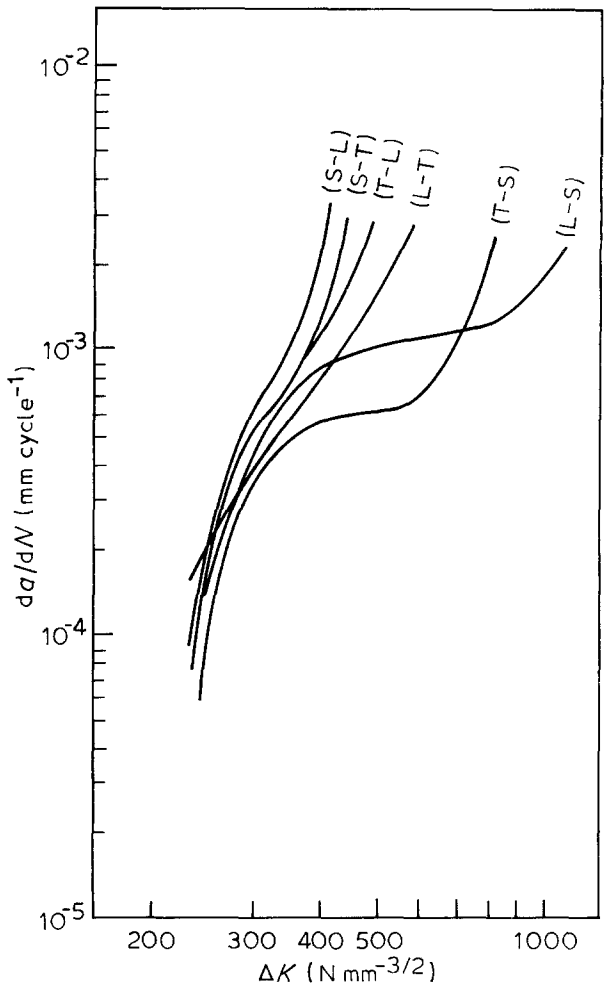

Figure 10 Third-degree polynomials fitted to da/dN against ΔK data of air fatigue tests in six orientations.

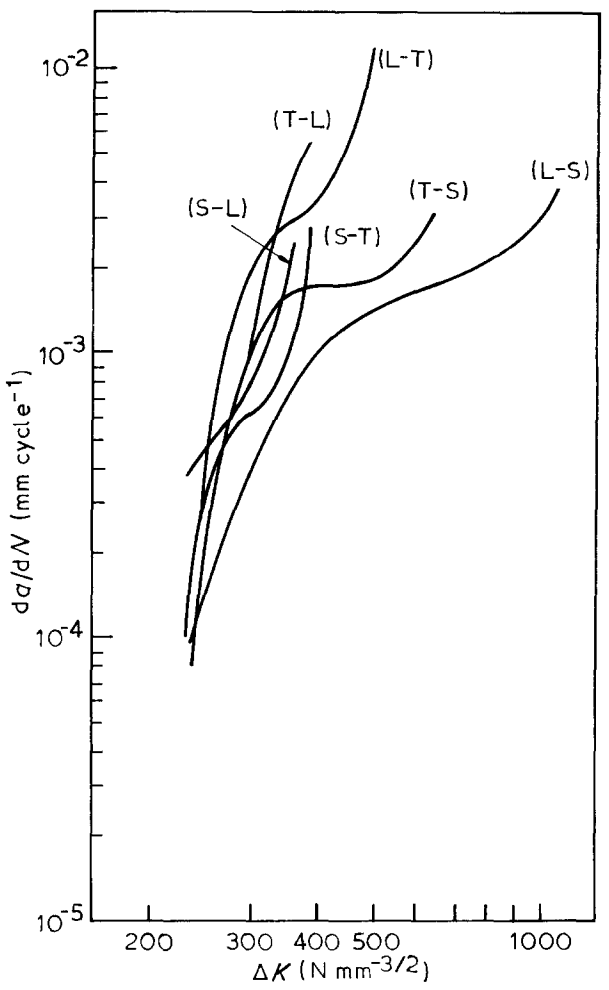

Figure 11 Third-degree polynomials fitted to da/dN against ΔK data of salt spray corrosion fatigue tests in six orientations.

4. Conclusions

The following conclusions can be drawn from the results of this investigation.

(1) The crack growth behaviour of the testing material is affected seriously by salt-water fog. Crack growth rates are greater by a factor 1.2 to 4.5 times compared to those of air tests. The severity of the effect of environment is found, however, to be dependent on the orientation.

(2) The fatigue life of the material in all orientations, decreases in salt-water fog relative to air.

(3) The crack growth behaviour of the material shows an important dependency on orientation. The material has lower resistance against fatigue crack growth, especially when the cracks propagate in the rolling direction.

(4) The L–S orientation should bē selected in the use of this material in both air and salt-water fog applications and the use of the S–L orientation should be avoided if possible.

Acknowledgements

This work was carried out within the frame of AGARD Additional Support Programme to South-Flank NATO Countries. The authors wish to express their thanks to the Turkish National Delegate at AGARD, to the Structure and Materials Panel of AGARD and to the Industrianlagen-Betriebsgesellschaft mbH, Ottobrunn, West Germany which supplied the 7050 aluminium alloy, for their generous support of this research.

References

1. L. F. MONDOLFO, in "Al-Alloys Structure and Properties", (Butterworths, London, 1976), p. 842.
2. Report No: TF-621.3, "Materials Research on Specific Components; Studies on Fracture Toughness and Fatigue Behavior of 7050 T73651 Semi-Product", IABG, West Germany, 1976.
3. ASTM E 647-83 (American Society for Testing and Materials, Philadelphia, 1983).
4. J. EFTIS, L. D. JONES and H. LIEBOWITZ in AGARDograph No. 176, "Fracture Mechanics of Aircraft Structures", 1974, edited by H. Liebowitz, p. 32.
5. A. CIGADA, B. MAZZA, T. PASTORE and P. PEDEFERRI, in Proceedings of an International Conference on HSLA Steels '85, China, November 1985 (ASM, Beijing, 1985).
6. M. O. SPEIDEL, "Stress Corrosion and Corrosion Fatigue Crack Growth in Al Alloys", Paper prepared for NATO ASI on SCC, Copenhagen, July 1975.
7. A. CIGADA, M. P. D'AMBROSIO, T. PASTORE and P. PEDEFERRI, in Proceedings of the 5th International Offshore Mechanics and Arctic Eng. Symposium, Vol 2 (ASME, 1986) p. 262.
8. D. ALIAGA and E. BUDILLON, in AGARD Conference Proceedings No. 316, "Corrosion Fatigue, Behaviour of Some Aluminium Alloys", Turkey, April 1982, 3-1.
9. D. J. DUQUETTE, in AGARD Conference Proceedings No. 316, "Mechanism of Corrosion Fatigue of Aluminium Alloys", Turkey, April 1982, 1-1.

Received 6 November 1989
and accepted 6 March 1990